World Journal of Advanced Research and Reviews
eISSN: 2581-9615 CODEN (USA): WJARAI
Cross Ref DOI: 10.30574/wjarr
Journal homepage: https://wjarr.com/

(RESEARCH ARTICLE)

Check for updates

Magnetohydrodynamic forced convection and heat transfer of a Casson fluid flow in an anisotropic porous channel with Isoflux boundaries

Chigozie Israel-Cookey, Onengiyeofori Anthony Davies * and Aminayanasa Paddy Ngeri

Department of Physics, Rivers State University, Nkpolu-Oroworukwo, Port Harcourt, Rivers State, Nigeria.

World Journal of Advanced Research and Reviews, 2023, 18(03), 1332–1347

Publication history: Received on 09 May 2023; revised on 25 June 2023; accepted on 27 June 2023

Article DOI: https://doi.org/10.30574/wjarr.2023.18.3.1214

Abstract

Theoretical analysis of magnetohydrodynamic fully developed forced convective flow and heat transfer characteristics of a non-Newtonian electrically conducting Casson fluid through a porous channel filled with anisotropic porous material bounded by two impermeable horizontal walls subject to constant heat flux applied to the outer walls is investigated. The extended Darcy-Brinkmann model govern the flow inside the porous channel and accounts for the presence of the inertia term, which allows for the no-slip boundary conditions at the walls. The principal axis of anisotropic permeability is oriented from **0** to $\frac{\pi}{2}$ radians. The equations governing the system are solved using the inbuilt "DSolve" in Mathematica 11.1 for the velocity and temperature profiles as well as the Nusselt number ($\boldsymbol{Nu}$), which characterizes the rate of heat transfer in the system. The effects of various parameters on the velocity, temperature and heat transfer profiles are displayed through graphs and discussed quantitatively. From the results we observed that the velocity profile reduced as the Casson parameter (β), anisotropic ratio (K_r), orientation angle (φ), and Hartmann number (Ha) increased, whereas the velocity profile increased when the Darcy number (Da) and apparent viscosity (λ) increased. Similarly, these variables also had similar effect on the temperature profile of the fluid. On the other hand, the heat transfer profile, as measured by Nusselt number, increased when the Casson parameter (β), anisotropic ratio (K_r) and Hartmann number (Ha) increased, while increasing the orientation angle (φ) and apparent viscosity (λ) decreased the Heat Transfer Profile. Upon further investigation, the heat transfer profile was shown to be maximum along the path of least permeability in the anisotropic porous media under investigation.

Keywords: Magnetohydrodynamic; Convection; Isoflux; Anisotropic; Porous; Darcy; Hartmann; Casson; Nusselt.

1. Introduction

Generally, any fluid whose viscosity changes relative to being strained by shear forces is said to be a non-Newtonian fluid [1]. A class on non-Newtonian fluids that is characterized by infinite viscosity at zero shear stress (a yield stress below which the fluid will not flow) and zero viscosity at infinite shear stress is known as Casson fluid [2]. In other words, Casson fluid are a class of non-Newtonian fluids that will only flow when it experiences a shear stress that is greater than its yield stress, otherwise it will behave like a solid [3]. Casson fluid has become quite popular amongst researchers in recent times as it has a wide range of application in such fields as metallurgy, drilling, food processing and bioengineering [4, 5].

Amongst the known non-Newtonian fluid models, successes in theoretical and experimental research [6, 7] have resulted in making the Casson fluid model, first introduced by Casson [8], well-accepted. To this effect, the flow of Casson fluids have been studied in different geometries by many researchers [4, 9, 10, 11, 12]. Additionally, many authors [13, 14, 15] have characterized the flow of non-Newtonian fluids relative to certain parameters that have the tendency of influencing their flow pattern.

* Corresponding author: Onengiyeofori A. Davies

Of recent, magnetohydrodynamic (MHD) convection flow has become a topic of discussion amongst researches due to its role in industrial and technological advancements [16]. This is because in electrically conducting fluids, there is a reduction in fluid velocities since convective currents are overcome by the Lorentz force [17]. It therefore means that the introduction of an external magnetic field can come in handy in maintaining convective currents, and hence, maintain fluid velocity in material industry [18].

Hayat *et. al.* [19] presented findings after studying Soret and Dufour effects on the magnetohydrodynamic (MHD) flow of the Casson fluid over a stretched surface. They estimated numerical values of Casson parameter, Hartman number and Prandtl number for different values of physical parameters (velocity, temperature and concentration fields). They showed that the temperature, the concentration, and the boundary layer thickness decrease by increasing the Prandtl number. Also, increases in Casson parameter and Hartman number had a diminishing effect on velocity profile while enhancing the temperature and concentration profile.

Mukhopadhyay *et. al.* [20] investigated the unsteady two-dimensional flow of Casson fluid over a stretching surface, having a prescribed temperature, relative to unsteadiness parameter (Casson parameter and Prandtl number) on velocity and temperature fields. They concluded that fluid velocity and temperature decrease relative to an increase in Prandtl number while increase in Casson parameter enhanced temperature while suppressing the velocity field.

Shehzad *et. al.* [21] investigated the effect of mass transfer in the magnetohydrodynamic flow of a Casson fluid over a porous stretching sheet in the presence of a chemical reaction. They showed that the Casson parameter and Hartman number have similar effects on the velocity in a qualitative sense, with concentration profile decreasing rapidly in comparison to the fluid velocity when there is an increase in the values of the suction parameter.

Ullah *et. al.* [22] carried out numerical analysis to investigate the effect of first order chemical reaction and thermal radiation on mixed convective flow of Casson fluid in the presence of magnetic field. They showed that fluid velocity rises with increase in radiation parameter in the case of assisting flow and is opposite in the case of opposing fluid while radiation parameter has no effect on fluid velocity in the forced convection. They also showed that fluid velocity and concentration were enhanced in the case generative chemical reaction whereas both profiles reduced in the case of destructive chemical reaction, with further increase in local unsteadiness parameter diminishing fluid velocity, temperature and concentration.

In their work, Tamoor *et. al.* [16] characterized Newtonian heating in MHD flows of Casson liquid induced by a stretched cylinder moving with linear velocity, with dissipation and Joule heating descriptive of the heat transfer process. They showed that velocity and thermal fields have reverse behavior for larger Hartman number. Moreover, curvature parameters have similar influence on the velocity, temperature, skin friction and Nusselt number.

Kumar *et. al.* [23] carried out extensive research to characterize the steady boundary layer stagnation flow of a Casson fluid over a stretching sheet with slips boundary conditions in the presence of viscous dissipation, Joule heating and the first order destructive chemical reaction. Amongst other findings, they showed that velocity, temperature and concentration decreased with an increase of velocity slip, thermal slip and solutal slip parameters.

Julien *et. al.* [24] studied the effect of magnetic field on convection heat transfer through packed porous beds which consists of a horizontal fluid layer (riverbed) and a porous zone with anisotropic permeability and underlined by a surface heated by a constant temperature. They analytically investigated how Hartmann number and hydrodynamic anisotropy controls the convective process. According to them, the magnetic field, anisotropic permeability and the thickness of the porous lining have a strong influence on the geothermal convective flow and the heat transfer rate.

Additionally, Anwar *et. al.* [25] examined the unsteady magnetohydrodynamic flow of a Casson fluid over an infinite vertical plate under ramped temperature and velocity conditions at the walls, incorporating thermal radiation flux and heat injection/suction terms in the energy equation. They showed that the magnetic field decelerates the flow, whereas the radiative flux leads to an upsurge in the flow. Furthermore, the shear stress is a decreasing function relative to the magnetic parameter.

Motivated by past research, this research is therefore geared towards theoretically analyzing the effect of magnetic field and Casson parameter on fully developed forced convective flow and heat transfer characteristics of a non-Newtonian electrically conducting Casson fluid through a porous channel filled with anisotropic porous material.

2. Methodology

The schematic diagram of the physical problem and coordinate system are shown in Figure 1.

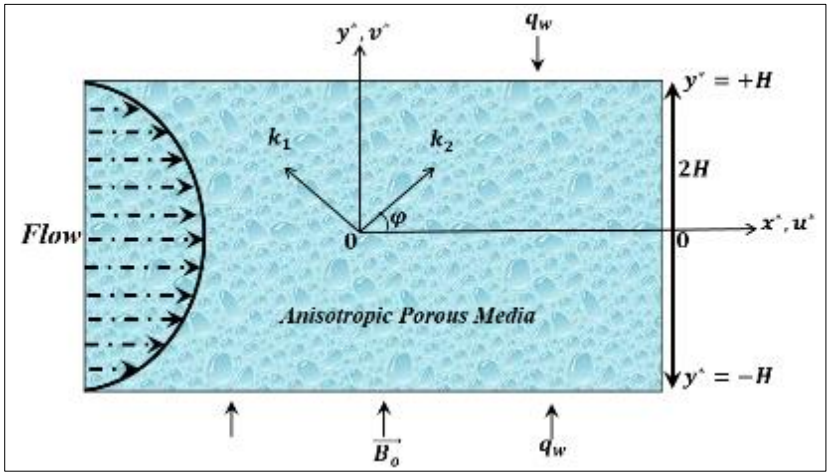

Figure 1 Schematic Diagram of the Physical Situation and Coordinate System

We consider an incompressible electrically conducting non-Newtonian Casson fluid flowing through a porous rectangular channel filled with anisotropic material. The horizontal channel is bounded by two impermeable walls located at $y^* = \pm H$ and are heated by a constant heat flux $q = \mathcal{K}\frac{\partial T^*}{\partial y^*}$. The flow is assumed to be steady and fully developed along the x^* direction and subjected to a uniform vertical magnetic field of strength $\overrightarrow{B_o}$.

Since the porous media is assumed to be anisotropic, the permeability k is a second order tensor described as Degan *et. al.* [26] and Karmakar *et. al.* [27];

$$k = \begin{pmatrix} k_1 \sin^2\varphi + k_2 \cos^2\varphi & (k_2 - k_1)\sin\varphi\cos\varphi \\ (k_2 - k_1)\sin\varphi\cos\varphi & k_2 \sin^2\varphi + k_1 \cos^2\varphi \end{pmatrix} \tag{1}$$

Where k_1 and k_2 are permeabilities along the two principal axes of the porous axes. The anisotropic porous media is characterized by the ratio $K_r = \frac{k_1}{k_2}$ and the orientation angle φ is defined as the angle between the horizontal direction and the principal axis with the permeability k_2.

The rheological equation of state for an incompressible flow of Casson fluid model is defined according to [28, 29],

$$\tau_{ij} = \begin{cases} \left(2\left(\mu_B + \frac{P_y}{\sqrt{2\pi}}\right)e_{ij}, \quad \pi > \pi_c\right) \\ \left(2\left(\mu_B + \frac{P_y}{\sqrt{2\pi_c}}\right)e_{ij} \quad \pi < \pi_c\right) \end{cases} \tag{2}$$

Where e_{ij} is the $(i,j)^{th}$ component of the deformation rate defined by,

$$e_{ij} = \frac{1}{2}\left(\frac{\partial V_i}{\partial x_j} + \frac{\partial V_j}{\partial x_i}\right), \qquad \pi = e_{ij}e_{ij} \tag{3a}$$

Also, π_C is the critical value of the value of this product based on the non-Newtonian model, μ_B is the plastic dynamic viscosity of the non-Newtonian fluid P_y is the yield stress of the field. When $\pi < \pi_C$, equation (2) can be expressed as,

$$\tau_{ij} = \mu_B\left(1 + \frac{1}{B}\right)(2e_{ij}) \tag{3b}$$

Where the Casson parameter, β, is defined as,

$$\beta = \frac{\mu_B}{P_y} \tag{3c}$$

Under the above considerations, together with the assumption that the induced magnetic and electric fields are negligible on the account of very small magnetic Reynolds number, the equations governing the steady, fully developed forced flow of an incompressible non-Newtonian Casson fluid in an anisotropic porous medium under the influence of vertical magnetic field are expressed by the equations of continuity (equation (4)), momentum (equation (5a) and (5b)) and energy (equation (6)) [26, 27, 28, 30].

$$\frac{du^*}{dx^*} = 0 \tag{4}$$

$$-\frac{\partial P^*}{\partial x^*} + \mu_{eff}\left(1 + \frac{1}{\beta}\right)\frac{d^2u^*}{dy^{*2}} - \frac{\mu}{k_1}au^* + \left(\vec{J} \times \overrightarrow{B_o}\right)_x = 0 \tag{5a}$$

$$-\frac{\partial p^*}{\partial x^*} - \frac{\mu}{k_1}cu^* = 0 \tag{5b}$$

$$\frac{\mathcal{K}}{(\rho C_p)_f}\frac{d^2T^*}{dy^{*2}} - u^*\frac{\partial T^*}{\partial x^*} = 0 \tag{6}$$

Where $a = \sin^2\varphi + k_r\cos^2\varphi$, $c = \frac{1}{2}(1 - k_r)\sin^2\varphi$. Also, $u^* = (u^*(y^*), 0)$ is the velocity component along the x^*-axis (since the flow is fully developed along the x^*-axis), P^* is the pressure, μ_{eff} is the effective viscosity of the fluid inside the porous media, μ is the dynamic viscosity, β is the Casson parameter, ρ is the density of the fluid, T^* is temperature, C_P is the heat capacity, $\mathcal{K}$ is the thermal conductivity, $\overrightarrow{B_o}$ is the uniform magnetic field, $\vec{J}$ is the current density and $(\vec{J} \times \overrightarrow{B_o})$ is the Lorentz force.

Assuming that the velocity and temperature fields are symmetric about the centre line of the channel, only the upper half of the channel is taken into consideration in the analysis that follows. Therefore, the appropriate boundary conditions are,

$$\frac{du^*}{dy^*} = 0, \frac{\partial T^*}{\partial y^*} = 0 \qquad on\ y^* = 0 \tag{7}$$

$$u^* = 0, \frac{\partial T^*}{\partial y^*} = \frac{q_w}{\mathcal{K}} \qquad on\ y^* = H^* \tag{8}$$

The Lorentz force $\left(\vec{J} \times \overrightarrow{B_o}\right)_x$ given in equation (5a) is such that,

$$\vec{J} = \sigma_C(\vec{E} + u^*B_o) \tag{9a}$$

Now assuming that $\vec{E} = (0,0,E_z)$, then,

$$\vec{J}_z = \sigma_C\left(\vec{E} + u^*B_o\right)_z \tag{9b}$$

For the steady flow fully developed Maxwell's equation $\vec{\nabla} \times \vec{E} = 0$, implying that $E_z = 0$ and equation (9b) reduces to,

$$\vec{J}_z = \sigma_C u^* B_o \tag{9c}$$

Hence,

$$\vec{J} \times \overrightarrow{B_o} = \left(\vec{J} \times \overrightarrow{B_o}\right) \times \overrightarrow{B_o} = -\sigma_C u^* B_o^2 \tag{9d}$$

Differentiating equations (5a) and (5b) partially with respect to x^*, using equation (4), yields,

$$\frac{\partial}{\partial x^*}\left(\frac{\partial P^*}{\partial x^*}\right) = 0 \tag{10a}$$

$$\frac{\partial}{\partial x^*}\left(\frac{\partial P^*}{\partial y^*}\right) = 0 \tag{10b}$$

According to Karmakar *et. al.* [27] and Nield *et. al.* [31], from equations (10a) and (10b), it follows that,

$$\frac{\partial P^*}{\partial x^*} = Constant = -G \tag{10c}$$

Using equations (9d) and (10c), the momentum equation can be rewritten as,

$$G + \mu_{eff}\left(1 + \frac{1}{\beta}\right)\frac{d^2u^*}{dy^{*^2}} - \frac{\mu}{k_1}au^* - \sigma_C u^* B_o^2 = 0 \tag{11}$$

2.1. Non-Dimensionalisation of the Governing Equations

We define the following non-dimensional variables to obtain the dimensionless form of equation (11),

$$y = \frac{y^*}{H}, u = \frac{\mu u^*}{GH^2} \tag{12}$$

By applying equation (12) to equations (6), (7), (8) and (11)

$$M\frac{d^2u}{dy^2} - M_1^2 u + 1 = 0 \tag{13}$$

$$u(1) = 0, \frac{du(0)}{dy} = 0 \tag{14}$$

where,

$M = \lambda\left(1 + \frac{1}{\beta}\right),\ M_1 = \left(\frac{a}{Da} + Ha^2\right)$

$Da = \frac{k_1}{H^2}$

$Ha = HB_o\sqrt{\frac{\sigma_c}{\mu}}$

$\lambda = \frac{\mu_{eff}}{\mu}$

From the above, Da is Darcy number, Ha is Hartmann number and λ is apparent viscosity. Since the flow is fully developed with constant heat flux at wall $y = 1$, and by the first law of thermodynamics [27, 31, 32],

$$\frac{dT_m^*}{dx^*} = \frac{1}{(\rho C_P)_f}\frac{q_m}{Hu_m^*} \tag{15}$$

Where u_m^* and T_m^* are respectively the bulk velocity and bulk temperature, defined as,

$$u_m^* = \frac{1}{H}\int_0^H u^*\, dy^* \tag{16a}$$

$$T_m^* = \frac{1}{Hu_m^*}\int_0^H u^* T^*\, dy^* \tag{16b}$$

Hence, the corresponding dimensionless bulk velocity is,

$$u_m = \int_0^1 u\, dy \tag{17}$$

Using equation (15) in equation (11),

$$\frac{u^*}{u_m^*} = \frac{\mathcal{K}H}{q_w}\frac{d^2T^*}{dy^{*2}} \tag{18}$$

In dimensionless form, equation (18) reduces to,

$$\frac{d^2\theta}{dy^2} + \frac{1}{2}Nu\, U = 0 \tag{19}$$

Subject to,

$$\theta(1) = 0, \qquad \frac{d\theta(0)}{dy} = 0 \tag{20}$$

Where we have used the following non-dimensionless variables,

$$U = \frac{u}{u_m}, \qquad \theta = \frac{T^* - T_w}{T_m - T_w}, \qquad Nu = \frac{2Hq_w}{\mathcal{K}(T^* - T_u^*)} \tag{21}$$

Here, Nu is the Nusselt number which characterizes the heat transfer between the wall and the porous media.

2.2. Solution to the Problem

Solving equation (13) subject to conditions presented in equation (14) yields the velocity profile of the system as,

$$u(y) = \frac{\cosh(\gamma) - \cosh(\gamma y)}{M_1^2\cosh(\gamma)}, \quad \gamma = \frac{M_1}{\sqrt{M}} \tag{22}$$

Using equation (22) in equation (17), the dimensionless bulk velocity becomes,

$$u_m = \int_0^1 u\, dy = \frac{M_1 - \sqrt{M}\tanh(\gamma)}{M_1^3} \tag{23}$$

And,

$$U(y) = \frac{[1 - \cosh(\gamma y)\,\mathrm{sech}(\gamma)]M_1}{M_1 - \sqrt{M}\tanh(\gamma)}, \quad U(y) = \frac{u(y)}{u_m} \tag{24}$$

Using equation (24) into (19) and solving with the help of conditions in equation (20), the result yields the temperature profile $\theta(y)$ as,

$$\theta(y) = \frac{\{2M\cosh(\gamma y) + \cosh(\gamma)[(1-y^2)M_1^2 - 2M]\}Nu}{4M_1\left\{M_1\cosh(\gamma) - \sqrt{M}\sinh(\gamma)\right\}}, \quad \gamma = \frac{M_1}{\sqrt{M}} \tag{25}$$

Having obtained the temperature profile $\theta(y)$ in equation (25), the Nusselt number, which characterizes the rate of convective heat transfer in the system is given by,

$$Nu = \frac{1}{\int_0^1 \Phi\, U\, dy} = \frac{12M_1\left\{M_1 - \sqrt{M}\tanh(\gamma)\right\}^2}{2M_1^2 + 15M^{\frac{3}{2}}\tanh(\gamma) - 3MM_1\{4 + \mathrm{sech}^2(\gamma)\}} \tag{26}$$

Here, we have used the compatibility condition according to Nield *et. al.* [31],

$$\int_0^1 \Phi\, U\, dy = 1 \tag{27}$$

And,

$$\Phi = \frac{2M\cosh(\gamma y) + \cosh(\gamma)[(1-y^2)M_1^2 - 2M]}{4M_1\left\{M_1\cosh(\gamma) - \sqrt{M}\sinh(\gamma)\right\}} \tag{28}$$

The velocity, temperature and heat transfer (Nusselt number) profiles as defined by equations 25, 28 and 26 will then be estimated for different values of Casson parameter (β), anisotropic ratio (K), Darcy number (Da), Hartman number (Ha), orientation angle (φ) and viscosity ratio (λ) to investigated how they are affected by these variables in the direction of the magnetic field from the center of the channel to the wall of the channel.

3. Results

3.1. Computation for Velocity Profile

The effect of varying the different variables on the temperature profile is shown in Figure 2.

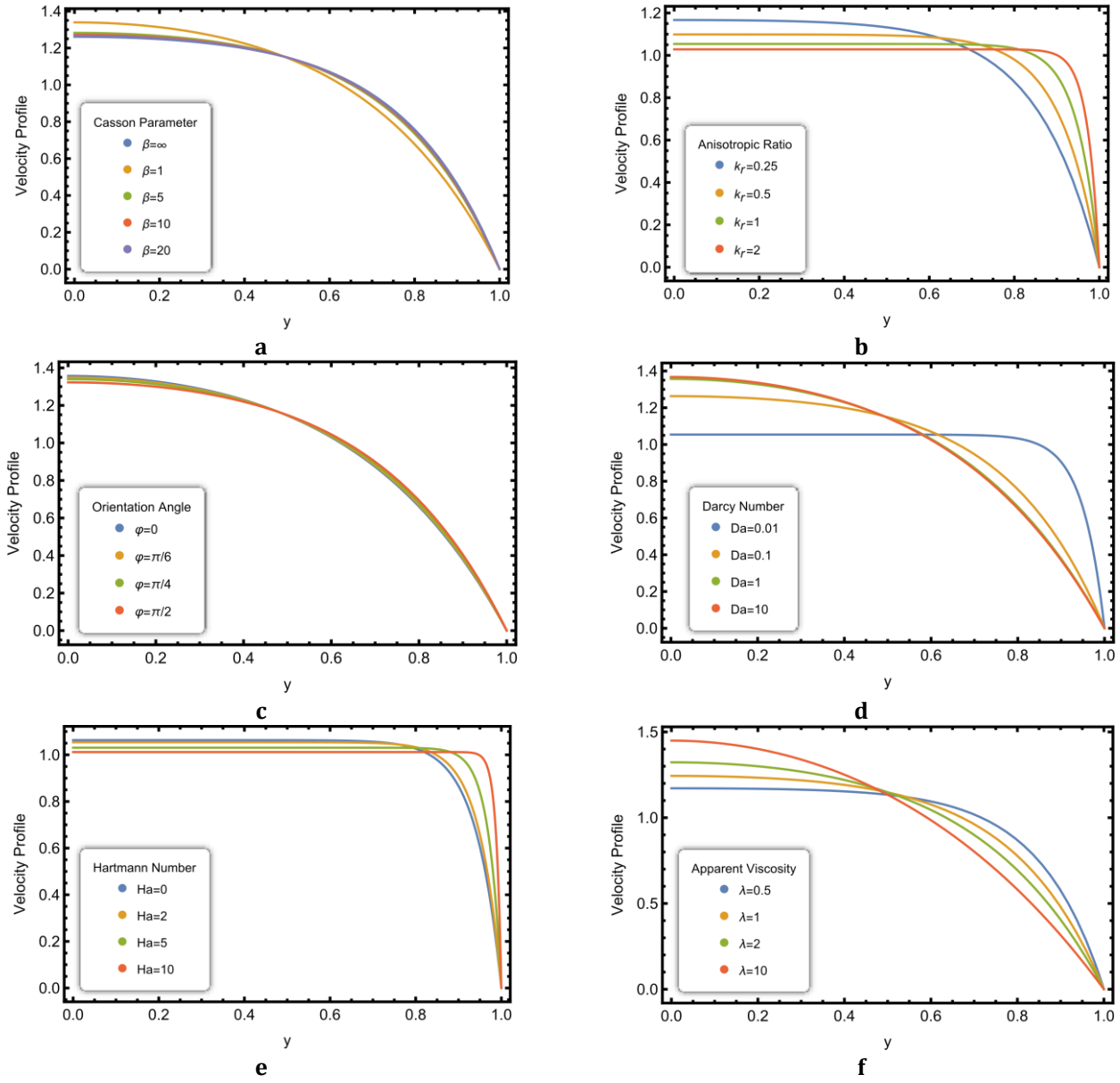

Figure 2 Velocity Profile for varying values of (a) Casson Parameter (b) Anisotropic ratio (c) Orientation angle (d) Darcy number (e) Hartmann number (f) Viscosity ratio

3.2. Computation for Temperature Profile

The effect of varying the different variables on the temperature profile is shown in Figure 3.

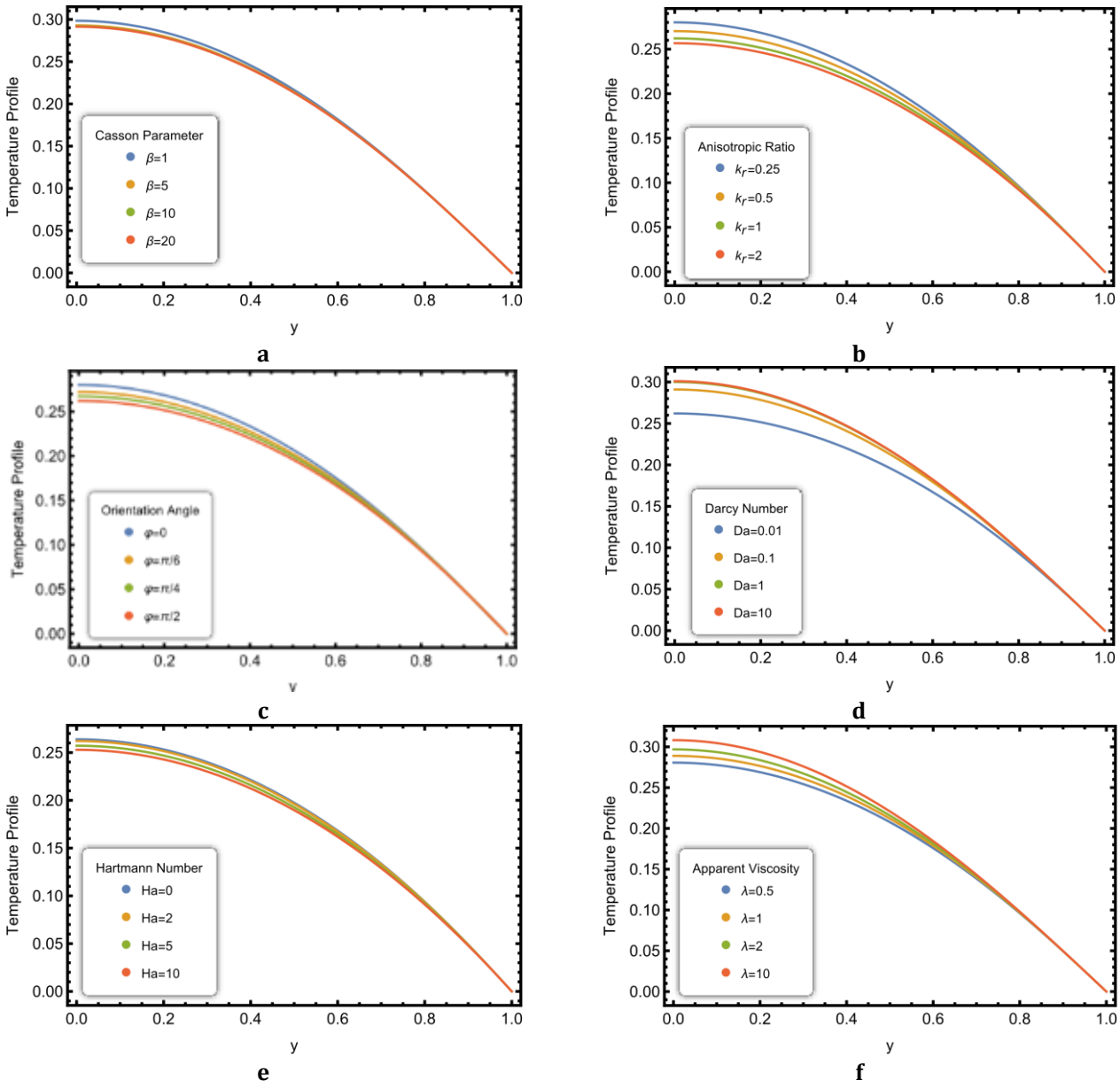

Figure 3 Temperature Profile for varying values of (a) Casson Parameter (b) Anisotropic ratio (c) Orientation angle (d) Darcy number (e) Hartmann number (f) Viscosity ratio

3.3. Computation for Heat Transfer (Nusselt Number) profile

The effect of varying the different variables on the heat transfer profile is shown in Figure 4.

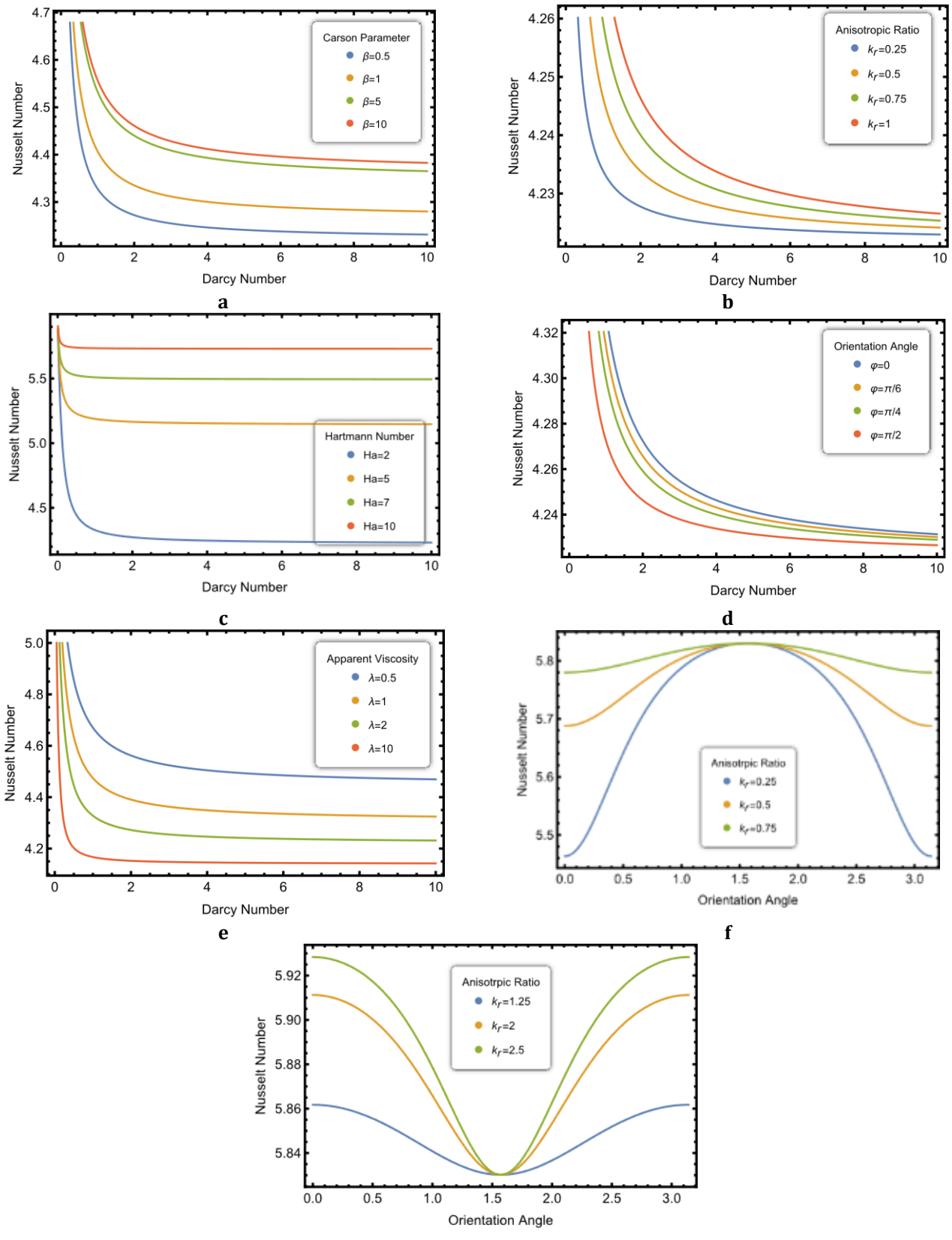

Figure 4 Heat transfer (Nusselt number) Profile for varying values of (a) Casson Parameter (b) Anisotropic ratio (c) Orientation angle (d) Hartmann number (e) Viscosity ratio (f) Anisotropic ratio ($K_r < 1$) with varying orientation angle (g) Anisotropic ratio ($K_r > 1$)with varying orientation angle

4. Discussion

4.1. Analysis of Velocity Profile

We maintained constant values of anisotropy ratio (0.25), Darcy number (1), Hartmann number (2), orientation angle (0) and apparent viscosity (2) while varying the values of Casson parameter ($\infty, 1, 5, 10, 20$) to investigate the effect of Casson parameter on the velocity profile as defined by equation 24. The result obtained is shown in Figure 2a. Generally, Casson parameter influences the velocity profile of non-Newtonian fluid by defining the dominance of yield stress against viscosity [33]. A greater Casson parameter implies a greater yield stress, indicating that a fluid requires a greater force to begin to flow. A lower Casson parameter, on the other hand, implies a lower yield stress, making the fluid easier to initiate flow. From the results obtained (Figure 2a), increasing the Casson parameter slightly decreased the velocity of the fluid at the center of the channel, probably because an increased Casson number is indicative of an increasing yield stress and therefore more force would be required to cause the fluid to flow. As can be seen in Figure 2, the velocity profile generally decreases vertically in the direction of the walls of the porous media, a phenomenon often referred to as velocity "shear thinning" or "wall effect" [34, 35], maximum in the middle of the flow channel and minimum at the walls. The result (Figure 2a) showed that increasing the Casson parameter delayed velocity shear thinning.

To further analyze the velocity profile, we maintained constant values of Casson parameter (10), Darcy number (0.04), Hartmann number (2), orientation angle (0) and apparent viscosity (2) while varying the values of anisotropic ratio (0.25, 0,5, 1, 2) to investigate the effect of anisotropic ratio on the velocity profile as defined by equation 24. The results, Figure 2b, showed that increasing the anisotropic ratio decreased the velocity profile while delaying velocity shear thinning. The reduction in velocity profile could be attributed to the fact that the alignment of particles or molecules in the direction of flow becomes more pronounced in a non-Newtonian fluid with a higher anisotropic ratio [36], thereby diminishing the fluid's flow velocity in the direction of alignment.

Furthermore, the effect of varying orientation angle of the flow channel on the fluid's velocity profile was also investigated. This was done by maintaining constant values of Casson parameter (10), anisotropic ratio (0.25), Darcy number (1), Hartmann number (2) and apparent viscosity (2) while varying the values of orientation angle ($0, \frac{\pi}{6}, \frac{\pi}{4}, \frac{\pi}{6}$) in equation 24. The result (Figure 2c) showed that increasing the angle of orientation of the flow channel slightly decreased the velocity profile with no visible effect on velocity shear thinning. This decrease in velocity profile relative to increasing angle of orientation could be attributed to either increased flow resistance [37] or altered shear rate distribution [38]. It is however important to note that the decrease in velocity profile with increasing orientation angle is typically modest, becoming more pronounced as the deviation from the channel walls increases according to Maynes *et. al.* [38].

The effect of Darcy number on the velocity of the fluid particle was also investigated by varying the values of Darcy number ($0.01, 0.1, 1, 10$) while maintaining constant values of Casson parameter (10), anisotropic ratio (0.25), Hartmann number (2), orientation angle (0) and apparent viscosity (2) in equation 24. The result (Figure 2d) showed that increasing Darcy number increased the velocity profile while enhancing velocity shear thinning. It is important to note that Darcy number, which describes fluid flow through porous media, has no direct influence on the velocity profile of a non-Newtonian fluid [39]. The increasing velocity profile with increasing Darcy number in our investigation could be attributed to the fact that an increasing Darcy number indicates increasing permeability of the porous media [31] offering less resistance to the fluid flowing through it and hence an increased velocity profile.

We also investigated the effect of Hartmann number on velocity profile by varying the values of Hartmann number ($0, 2, 5, 10$) while maintaining constant values of Casson parameter (10), anisotropic ratio (0.25), Darcy number (0.01), orientation angle (0) and apparent viscosity (2) in equation 24. The result (Figure 2e) showed that the increasing the Hartman number caused a reduction in the velocity profile while delaying velocity shear thinning. In fluid flow, the Hartmann number is defined as the ratio of magnetic forces to viscous forces [40]. It then implies that increasing the Hartmann number would be indicative of the fact that the flow profile is dominated by magnetic forces relative to viscous forces which should enhance the velocity profile of the fluid in the direction of flow. In this study however, the magnetic field is oriented perpendicularly to the direction of flow which could be a reason why increasing the Hartmann number is causing a reduction in the velocity profile of the fluid in the direction of the magnetic field.

The effect of apparent viscosity on the velocity profile was also investigated by varying the value of apparent viscosity ($0.5, 1, 2, 10$) while maintain constant values of Casson parameter (10), anisotropic ratio (0.25), Darcy number (0.01), Hartmann number (2) and orientation angle (0) in equation 24. The apparent viscosity of a non-Newtonian fluid is a measure of the shear stress to the corresponding shear rate [41]. Therefore, increasing the apparent viscosity will

indicate an increase in shear stress relative to shear rate which will in turn lead to the reduction of the viscosity of the non-Newtonian fluid and hence a reduction in the flow resistance offered by the fluid. Therefore, increasing the apparent viscosity will increase the velocity profile of the fluid as suggested by our result (Figure 2f).

4.2. Analysis of Temperature Profile

Furthermore, we maintained constant values of anisotropy ratio (0.25), Darcy number (1), Hartmann number (2), orientation angle (0) and apparent viscosity (2) while varying the values of Casson parameter $(\infty, 1, 5, 10, 20)$ to investigate the effect of Casson parameter on the temperature profile as defined by equation 25. The precise relationship between the Casson parameter and the temperature profile of a non-Newtonian fluid is dependent on the fluid's physical and thermal properties [42]. Changes in the Casson number might however have an indirect effect on the temperature profile in certain conditions [43]. In certain flow configurations, such as highly confined geometries (such as we have applied in this study) or complex flow regimes, an increasing Casson parameter may interact with other factors to diminish the effect on the temperature profile [44]. This could be the reason for the diminishing effect produced on the temperature profile with increasing Casson parameter as shown in Figure 3a.

To further analyze the temperature profile, we maintained constant values of Casson parameter (10), Darcy number (0.04), Hartmann number (2), orientation angle (0) and apparent viscosity (2) while varying the values of anisotropic ratio (0.25, 0,5, 1, 2) to investigate the effect of anisotropic ratio on the temperature profile as defined by equation 25. As the anisotropic ratio increases, the fluid's properties become more directionally dependent. This can affect the thermal transfer characteristics of the fluid [45]. Non-Newtonian fluids that are anisotropic can therefore have different thermal conductivity or heat transfer along different planes or directions. In some circumstances, raising the anisotropy ratio can result in improved heat transport in specific directions or orientations over others. This can result in a decrease in temperature profile, especially in the direction or orientation where heat transport is most efficient. (Figure 3b).

Additionally, the effect of varying orientation angle of the flow channel on the fluid's temperature profile was also investigated. This was done by maintaining constant values of Casson parameter (10), anisotropic ratio (0.25), Darcy number (0.04), Hartmann number (2) and apparent viscosity (2) while varying the values of orientation angle $(0, \frac{\pi}{6}, \frac{\pi}{4}, \frac{\pi}{6})$ in equation 25. The result (Figure 3c) showed that increasing the angle of orientation of the flow channel reduces the temperature profile by flattening it. Flow characteristics, such as flow patterns and velocity distribution, can be affected by the flow channel's tilt or inclination. Since increasing the orientation of the flow channel reduces the velocity profile as already shown, this could lead to a decrease in the temperature profile of the fluid since, in some cases [46], the velocity and temperature profiles of non-Newtonian fluids have a direct relationship.

The effect of Darcy number on temperature profile was also investigated by varying the values of Darcy number $(0.01, 0.1, 1, 10)$ while maintaining constant values of Casson parameter (10), anisotropic ratio (0.25), Hartmann number (2), orientation angle (0) and apparent viscosity (2) in equation 25. The result (Figure 3d) showed that increasing Darcy number increased the temperature profile. Typically, a rise in the Darcy number corresponds to a rise in the flow velocity through the porous medium, as we have already shown. Higher flow velocities can improve convective heat transfer, resulting in greater heat transfer rates [46]. This can result in enhancing the temperature profile as seen from our result.

To further analyze the temperature profile, we investigated the effect of Hartmann number on the temperature profile by varying the values of Hartmann number $(0, 2, 5, 10)$ while maintaining constant values of Casson parameter (10), anisotropic ratio (0.25), Darcy number (0.01), orientation angle (0) and apparent viscosity (2) in equation 25. The result (Figure 3e) showed that the increasing the Hartman number caused a reduction in the temperature profile. In MHD systems, a strong magnetic field can inhibit fluid motion and impede thermal transport [47]. As the Hartmann number rises, magnetic forces become stronger relative to viscous forces, resulting in increased flow suppression and diminished thermal mixing. This, in turn, results in a fluid with a more confined temperature distribution as can be seen in our results.

We also investigated the effect of apparent viscosity on the temperature profile by varying the value of apparent viscosity (0.5, 1, 2, 10) while maintain constant values of Casson parameter (10), anisotropic ratio (0.25), Darcy number (0.01), Hartmann number (2) and orientation angle (0) in equation 25. The result (Figure 3f) showed that increasing the apparent viscosity produced an increase in the temperature profile. We had already stated that an increase I apparent viscosity is indicative of an increase in shear stress experienced by the fluid which will produce greater velocity gradients. This could also lead to a more pronounced deformation of the fluid [48]. The fluid's temperature rises because of the increased dissipation of mechanical energy caused by the increased shear stress [49]. This could be the reason why the temperature profile is increasing with apparent viscosity in our result.

4.3. Analysis of Heat Transfer (Nusselt Number) profile

The Nusselt number (Nu) describes the efficiency of heat transport as well as the relative contributions of conduction and convection to the heat transfer mechanism in during fluid motion [50]. When the Nusselt number is considered in a direction perpendicular to the direction of flow, like we have done in this study, it reflects the heat transfer that occurs owing to conduction between the solid and the surrounding fluid [51]. When the Darcy number rises, it usually suggests that fluid movement through porous media is becoming more difficult. This increased resistance in non-Newtonian fluids can result in different flow patterns, larger pressure drops, and increased viscous dissipation within the fluid [52]. Additionally, increased viscous dissipation can cause local heating of the fluid, affecting temperature distribution within the porous media. This altered temperature distribution has the potential to change the temperature gradients perpendicular to the flow direction, thus impeding heat conduction in that direction. This is reflected in our result (Figure 4). However. we analyzed the heat transfer (Nusselt number) profile by varying our variables of interest relative to an increasing Darcy number to investigate how these variables affected the dampening effect of an increasing Darcy number (0.01 to 10) on the Heat transfer profile.

We began by maintaining constant values of anisotropy ratio (2), Hartmann number (2) orientation angle (0) and apparent viscosity (2) while varying the values of Casson parameter (0.5,1, 5, 10) in equation 24. The results (Figure 4a) showed that increasing the Casson parameter enhanced the heat transfer profile perpendicular to flow direction. The non-Newtonian behavior brought on by an increasing Casson parameter may prevent the thermal boundary layer from forming and expanding, resulting in better heat transmission perpendicular to the flow direction [53]. This disturbance can improve convective heat transfer by bringing new fluid into touch with the solid boundaries, allowing heat to be carried away more effectively. This could be the reason for the enhanced heat transfer profile relative to increased Casson parameter as suggested by our result.

Furthermore, while maintaining constant values of Casson parameter (0.5), Hartmann number (2) orientation angle (0) and apparent viscosity (2), we varied the values of anisotropic ratio (0.25,0.5, 0.75, 1) in equation 24. The results (Figure 4b) showed that increasing the anisotropic ratio enhanced the heat transfer profile perpendicular to flow direction. Wang *et. al.* [54] showed that fluid may experience vortices, eddies, or whirling motions due to the anisotropic aspect of the flow, which enhances fluid mixing. By enhancing the interaction between the fluid and solid boundaries perpendicular to the flow direction, this improved mixing can promote better heat transmission, as suggested by our result.

Additionally, we analyzed the effect of increasing Hartmann number (0,2,5,7,10) on the Nusselt number by maintaining constant values of Casson parameter (0.5), anisotropic ratio (2) orientation angle (0) and apparent viscosity (2) in equation 24, The result (Figure 4c) showed that heat transfer by conduction was enhanced with increasing Hartmann number. Zhang *et. al.* [55] had shown in their research that it is quite possible that flow instabilities or changes in the flow structure in a non-Newtonian fluid could be initiated when the non-Newtonian fluid interacts with a magnetic field. The heat transfer profile may be impacted by these flow instabilities, which would improve heat transfer perpendicular to the flow direction, hence enhanced heat transfer in that direction as shown by our result.

We also investigated how the angle of orientation of the flow channel affected the heat transfer profile as defined by Nusselt number. This was done by maintaining constant values of Casson parameter (0.5), anisotropic ratio (2) Hartmann number (2) and apparent viscosity (2) while varying the angle of orientation $(0, \frac{\pi}{6}, \frac{\pi}{4}, \frac{\pi}{6})$ in equation 24. The result, Figure 4d, showed that an increasing angle of orientation diminished the temperature profile perpendicularly to the direction of flow. In the porous media, flow separation or recirculation zones can be facilitated by higher angles of orientation [56]. As a result of these flow patterns, there may be less heat transmission across the fluid-solid interfaces which could be the reason for the nature of our result.

Finally, the effect of apparent viscosity on the heat profile was also investigated in this study. To achieve this, we varied the values of apparent viscosity (0.5,1,2,10) while maintaining constant values of Casson parameter (0.5), anisotropic ratio (2) Hartmann number (2) and orientation angle (2). The result (Figure 4e) showed that increasing the apparent viscosity reduced the heat transfer profile. In some circumstances, a rise in apparent viscosity can encourage flow channeling, in which the fluid favors going down particular lanes or channels [57]. This flow channeling tendency can limit heat transmission perpendicular to the flow direction and decrease the overall heat transfer area which could be the reason for our obtained result.

Since anisotropic ratio is very vital in describing the dynamics of an anisotropic porous media according to Shin [58], we also investigated the effect of varying anisotropic ratio ($K_r < 1$ and $K_r > 1$) with varying orientation angle (0 to π) on the heat transfer profile. For $K_r < 1$, i.e. the permeability along the principal axis parallel to the direction of flow is

lower than the permeability along the principal axis perpendicular to the direction of flow, the result (Figure 4f) showed that the heat transfer was maximum when the orientation angle is 90^o $(\frac{\pi}{2})$, along the principal axis. and minimum when the angle of orientation was 0 and 180^o (π), along the direction of flow. The opposite scenario was however observed (Figure 4g) for $K_r > 1$, i.e. when the permeability along the principal axis parallel to the direction of flow is higher than the permeability along the principal axis perpendicular to the direction of flow. This was similar to results obtained by Degan *et. al.* [26]. Evidently therefore, the heat transfer profile is maximum along the least permeable path. This could be because the least permeable path offers the highest resistance to heat flow. This resistance causes the temperature gradient along this path to be steeper, resulting in a higher rate of heat transfer, a phenomena known as the "bottleneck effect" that is widely observed in porous media [59].

5. Conclusion

We have theoretically investigated the heat transfer characteristics and magnetohydrodynamic fully developed forced convective flow of a non-Newtonian electrically conducting Casson fluid through a porous channel filled with anisotropic porous material and bounded by two impermeable horizontal walls under constant heat flux applied to the outer walls. We characterized the effect of varying Casson parameter (β), anisotropic ratio (K_r), Darcy number (Da), Hartmann number (Ha), angle of orientation (φ) and apparent viscosity (λ) on the velocity, temperature and heat transfer (Nusselt) number profiles of the non-Newtonian fluid in a direction perpendicular to the direction of fluid flow. The result obtained showed that.

- Increasing the Casson parameter (β), anisotropic ratio (K_r), orientation angle (φ) and Hartmann number (Ha) decreased the velocity profile while increasing the Darcy number (Da) and apparent viscosity (λ) increased the velocity profile.
- Increasing the Casson parameter (β), anisotropic ratio (K_r), orientation angle (φ) and Hartmann number (Ha) decreased the velocity profile while increasing the Darcy number (Da) and apparent viscosity (λ) increased the temperature profile.
- Increasing the Casson parameter (β), anisotropic ratio (K_r) and Hartmann number (Ha) increased the Heat transfer profile as defined by Nusselt number while increasing the orientation angle (φ) and apparent viscosity (λ) decreased the Heat transfer profile.
- The heat transfer profile was maximum along the least permeable path.

Compliance with ethical standards

Acknowledgments

The authors are thankful to the Vice Chancellor, Rivers State University, Port Harcourt, for providing the resources needed for the completion of this research work.

Disclosure of conflict of interest

The authors declare that there are no conflicts of interest.

References

[1] Irgens, F., *Rheology and Non-Newtonian Fluids*. Vol. 1. 2014: Springer.

[2] Pramanik, S., *Casson Fluid Flow and Heat Transfer Past an Exponentially Porous Stretching Surface in Presence of Thermal Radiation.* Ain Shams Engineering Journal, 2014. **5**(1): p. 205-212.

[3] El-Zahar, E.R., A.E.N. Mahdy, A.M. Rashad, W. Saad, and L.F. Seddek, *Unsteady MHD Mixed Convection flow of Non-Newtonian Casson Hybrid Nanofluid in the Stagnation Zone of Sphere Spinning Impulsively.* Fluids, 2021. **6**(6): p. 197.

[4] Ramesh, K. and M. Devakar, *Some Analytical Solutions for flows of Casson Fluid with Slip Boundary Conditions.* Ain Shams Engineering Journal, 2015. **6**(3): p. 967-975.

[5] Reddy, S.B.V., D.P. Ashwathnarayana, J. Mysore, and D.V. Chandrashekhar, *Ohmic and Viscous Dissipation Effect on Free and Forced Convective Flow of Casson Fluid in a Channel.* Biointerface Research in Applied Chemistry, 2021. **12**(1): p. 132-148.

[6] Sharp, M.K., *Shear-Augmented Dispersion in Non-Newtonian Fluids.* Annals of Biomedical Engineering, 1993. **21**(4): p. 407-415.

[7] Nadeem, S., R.U. Haq, and C. Lee, *MHD Flow of a Casson Fluid over an Exponentially Shrinking Sheet.* Scientia Iranica, 2012. **19**(6): p. 1550-1553.

[8] Casson, N., *A Flow Equation for Pigment-Oil Suspensions of the Printing Ink type.* Rheology of Disperse Systems, 1959: p. 84-104.

[9] Chevalley, J., *An Adaptation of the Casson Equation for the Rheology of Chocolate.* Journal of Texture Studies, 1991. **22**(2): p. 219-229.

[10] Kirsanov, E.A. and S.V. Remizov, *Application of the Casson Model to Thixotropic Waxy Crude Oil.* Rheologica acta, 1999. **38**(2): p. 172-176.

[11] Sankar, D. and U. Lee, *FDM Analysis for MHD Flow of a Non-Newtonian Fluid for Blood Flow in Stenosed Arteries.* Journal of Mechanical Science & Technology, 2011. **25**(10): p. 2573-2581.

[12] Oke, A.S., W.N. Mutuku, M. Kimathi, and I.L. Animasaun, *Insight into the Dynamics of Non-Newtonian Casson Fluid over a Rotating Non-Uniform Surface Subject to Coriolis Force.* Nonlinear Engineering, 2020. **9**(1): p. 398-411.

[13] Hayat, T., M. Hussain, S. Nadeem, and S. Mesloub, *Falkner–Skan Wedge Flow of a Power-Law Fluid with Mixed Convection and Porous Medium.* Computers & Fluids, 2011. **49**(1): p. 22-28.

[14] Nadeem, S., R.U. Haq, and N.S. Akbar, *MHD Three-Dimensional Boundary Layer Flow of Casson Nanofluid past a Linearly Stretching Sheet with Convective Boundary Condition.* IEEE Transactions on Nanotechnology, 2013. **13**(1): p. 109-115.

[15] Raju, C. and N. Sandeep, *Heat and Mass Transfer in MHD Non-Newtonian Bio-Convection Flow over a Rotating Cone/Plate with Cross Diffusion.* Journal of Molecular Liquids, 2016. **215**: p. 115-126.

[16] Tamoor, M., M. Waqas, M.I. Khan, A. Alsaedi, and T. Hayat, *Magnetohydrodynamic Flow of Casson Fluid over a Stretching Cylinder.* Results in Physics, 2017. **7**: p. 498-502.

[17] Mahapatra, T.R., D. Pal, and S. Mondal, *Mixed Convection Flow in an Inclined Enclosure under Magnetic Field with Thermal Radiation and Heat Generation.* International Communications in Heat and Mass Transfer, 2013. **41**: p. 47-56.

[18] Hayat, T., Z. Hussain, A. Alsaedi, and T. Muhammad, *An Optimal Solution for Magnetohydrodynamic Nanofluid Flow over a Stretching Surface with Constant Heat Flux and Zero Nanoparticles Flux.* Neural Computing Applications, 2018. **29**(12): p. 1555-1562.

[19] Hayat, T., S. Shehzad, and A. Alsaedi, *Soret and Dufour Effects on Magnetohydrodynamic (MHD) Flow of Casson Fluid.* Applied Mathematics and Mechanics, 2012. **33**(10): p. 1301-1312.

[20] Mukhopadhyay, S., P.R. De, K. Bhattacharyya, and G. Layek, *Casson Fluid Flow over an Unsteady Stretching Surface.* Ain Shams Engineering Journal, 2013. **4**(4): p. 933-938.

[21] Shehzad, S., T. Hayat, M. Qasim, and S. Asghar, *Effects of Mass Transfer on MHD Flow of Casson Fluid with Chemical Reaction and Suction.* Brazilian Journal of Chemical Engineering, 2013. **30**(1): p. 187-195.

[22] Ullah, I., K. Bhattacharyya, S. Shafie, and I. Khan, *Unsteady MHD Mixed Convection Slip Flow of Casson Fluid Over Nonlinearly Stretching Sheet Embedded in a Porous Medium with Chemical Reaction, Thermal Radiation, Heat Generation/Absorption and Convective Boundary Conditions.* PloS one, 2016. **11**(10): p. e0165348.

[23] Kumar, G.V., R.K. Kumar, and S. Varma, *Multiple Slips and Chemical Reaction Effects on MHD Stagnation Point Flow of Casson Fluid over a Stretching Sheet with Viscous and Joules Heating.* Frontiers in Heant and Mass Transfer, 2018. **10**(23).

[24] Julien, Y., D. Gérard, and F. Latif, *Effect of Constant Magnetic Field on Convective Heat Transfer through Anisotropic River Beds.* Journal of Crystallization Process and Technology, 2018. **8**: p. 57-71.

[25] Anwar, T., P. Kumam, and W. Watthayu, *Unsteady MHD Natural Convection Flow of Casson Fluid Incorporating Thermal Radiative Flux and Heat Injection/Suction Mechanism under Variable Wall Conditions.* Scientific Reports, 2021. **11**(1): p. 1-15.

[26] Degan, G., S. Zohoun, and P. Vasseur, *Forced Convection in Horizontal Porous Channels with Hydrodynamic Anisotropy.* International Journal of Heat and Mass Transfer, 2002. **45**(15): p. 3181-3188.

[27] Karmakar, T., M. Reza, and G.R. Sekhar, *Forced convection in a fluid saturated anisotropic porous channel with isoflux boundaries.* Physics of Fluids, 2019. **31**(11): p. 117109.

[28] Bukhari, Z., A. Ali, Z. Abbas, and H. Farooq, *The pulsatile flow of thermally developed non-Newtonian Casson fluid in a channel with constricted walls.* AIP Advances, 2021. **11**(2): p. 025324.

[29] Qawasmeh, B.R., M. Alrbai, and S. Al-Dahidi, *Forced convection heat transfer of Casson fluid in non-Darcy porous media.* Advances in Mechanical Engineering, 2019. **11**(1): p. 1687814018819906.

[30] Ali, M.F., K. Naganthran, R. Nazar, and I. Pop, *MHD mixed convection boundary layer stagnation-point flow on a vertical surface with induced magnetic field: A stability analysis.* nternational Journal of Numerical Methods for Heat & Fluid Flow, 2020. **30**(11): p. 4697-4710.

[31] Nield, D.A., S. Junqueira, and J.L. Lage, *Forced convection in a fluid-saturated porous-medium channel with isothermal or isoflux boundaries.* Journal of Fluid Mechanics, 1996. **322**: p. 201-214.

[32] Bejan, A., *Advanced engineering thermodynamics*. 2016: John Wiley & Sons.

[33] Rao, A.S., V.R. Prasad, K. Harshavalli, and O.A. Beg, *Thermal radiation effects on non-Newtonian fluid in a variable porosity regime with partial slip.* Journal of Porous Media, 2016. **19**(4).

[34] Bhatti, M. and M.A. Abbas, *Simultaneous effects of slip and MHD on peristaltic blood flow of Jeffrey fluid model through a porous medium.* Alexandria Engineering Journal, 2016. **55**(2): p. 1017-1023.

[35] Amaratunga, M., H.A. Rabenjafimanantsoa, and R.W. Time, *Influence of low-frequency oscillatory motion on particle settling in Newtonian and shear-thinning non-Newtonian fluids.* Journal of Petroleum Science and Engineering, 2021. **196**: p. 107786.

[36] Cunha, F. and D. Albernaz, *Oscillatory motion of a spherical bubble in a non-Newtonian fluid.* Journal of Non-Newtonian fluid mechanics, 2013. **191**: p. 35-44.

[37] Azinfar, H. and J.A. Kells, *Flow resistance due to a single spur dike in an open channel.* Journal of Hydraulic research, 2009. **47**(6): p. 755-763.

[38] Maynes, D., K. Jeffs, B. Woolford, and B. Webb, *Laminar flow in a microchannel with hydrophobic surface patterned microribs oriented parallel to the flow direction.* Physics of fluids, 2007. **19**(9): p. 093603.

[39] Pearson, J. and P. Tardy, *Models for flow of non-Newtonian and complex fluids through porous media.* Journal of Non-Newtonian Fluid Mechanics, 2002. **102**(2): p. 447-473.

[40] Afrand, M., *Using a magnetic field to reduce natural convection in a vertical cylindrical annulus.* International Journal of Thermal Sciences, 2017. **118**: p. 12-23.

[41] Partal, P. and J.M. Franco, *Non-Newtonian Fluids.* Rheology: Encyclopaedia of Life Support Systems , UNESCO. Eolss, Oxford, 2010: p. 96-119.

[42] Santoshi, P.N., G.V.R. Reddy, and P. Padma, *Flow features of non-newtonian fluid through a paraboloid of revolution.* International Journal of Applied and Computational Mathematics, 2020. **6**: p. 1-22.

[43] Jalili, P., A.A. Azar, B. Jalili, and D.D. Ganji, *Study of nonlinear radiative heat transfer with magnetic field for non-Newtonian Casson fluid flow in a porous medium.* Results in Physics, 2023. **48**: p. 106371.

[44] Basha, H., N.K. Nedunuri, G.J. Reddy, and S. Ballem, *Thermal analysis of buoyancy-motivated Casson fluid flow with time-independent chemical reaction under Lorentz forces.* Heat Transfer, 2021. **50**(7): p. 7291-7320.

[45] Mala, G.M., D. Li, and J. Dale, *Heat transfer and fluid flow in microchannels.* International Journal of Heat and Mass Transfer, 1997. **40**(13): p. 3079-3088.

[46] Shojaeian, M. and A. Koşar, *Convective heat transfer and entropy generation analysis on Newtonian and non-Newtonian fluid flows between parallel-plates under slip boundary conditions.* International Journal of Heat and Mass Transfer, 2014. **70**: p. 664-673.

[47] Bondareva, N.S. and M.A. Sheremet, *Natural convection heat transfer combined with melting process in a cubical cavity under the effects of uniform inclined magnetic field and local heat source.* International Journal of Heat and Mass Transfer, 2017. **108**: p. 1057-1067.

[48] Sochi, T., *Flow of non-Newtonian fluids in porous media.* Journal of Polymer Science Part B: Polymer Physics, 2010. **48**(23): p. 2437-2767.

[49] Chen, C.-H., *Effect of viscous dissipation on heat transfer in a non-Newtonian liquid film over an unsteady stretching sheet.* Journal of Non-Newtonian Fluid Mechanics, 2006. **135**(2-3): p. 128-135.

[50] Tagle-Salazar, P.D., K. Nigam, and C.I. Rivera-Solorio, *Heat transfer model for thermal performance analysis of parabolic trough solar collectors using nanofluids.* Renewable Energy, 2018. **125**: p. 334-343.

[51] Tiggelbeck, S., N. Mitra, and M. Fiebig, *Comparison of wing-type vortex generators for heat transfer enhancement in channel flows.* Experimental Thermal and Fluid Science, 1994. **5**(2): p. 425-436.

[52] Kostic, M., *On turbulent drag and heat transfer reduction phenomena and laminar heat transfer enhancement in non-circular duct flow of certain non-Newtonian fluids.* International Journal of Heat and Mass Transfer, 1994. **37**: p. 133-147.

[53] El-Dabe, N.T., A.Y. Ghaly, R.R. Rizkallah, K.M. Ewis, and A.S. Al-Bareda, *Numerical solution of MHD boundary layer flow of non-Newtonian Casson fluid on a moving wedge with heat and mass transfer and induced magnetic field.* Journal of Applied Mathematics and Physics, 2015. **3**(06): p. 649.

[54] Wang, P., X.-S. Bai, M. Wessman, and J. Klingmann, *Large eddy simulation and experimental studies of a confined turbulent swirling flow.* Physics of fluids, 2004. **16**(9): p. 3306-3324.

[55] Zhang, R., S. Aghakhani, A.H. Pordanjani, S.M. Vahedi, A. Shahsavar, and M. Afrand, *Investigation of the entropy generation during natural convection of Newtonian and non-Newtonian fluids inside the L-shaped cavity subjected to magnetic field: application of lattice Boltzmann method.* The European Physical Journal Plus, 2020. **135**(2): p. 184.

[56] Bég, O.A., L. Sim, J. Zueco, and R. Bhargava, *Numerical study of magnetohydrodynamic viscous plasma flow in rotating porous media with Hall currents and inclined magnetic field influence.* Communications in Nonlinear Science and Numerical Simulation, 2010. **15**(2): p. 345-359.

[57] Chen, Y.-S., C.-C. Lin, and H.-S. Liu, *Mass transfer in a rotating packed bed with viscous Newtonian and non-Newtonian fluids.* Industrial and Engineering Chemistry Research, 2005. **44**(4): p. 1043-1051.

[58] Shin, C.-H., *Alternative flow model of anisotropic porous media.* Journal of Natural Gas Science and Engineering, 2022. **108**: p. 104829.

[59] Swartzendruber, D., *Water flow through a soil profile as affected by the least permeable layer.* Journal of Geophysical Research, 1960. **65**(12): p. 4037-4042.